ELSEVIER

Surface Science 512 (2002) 151–164

SURFACE SCIENCE

www.elsevier.com/locate/susc

Analysis and theory of multilayer desorption: Ag on Re

S.H. Payne [a], J.M. LeDue [a], J.C. Michael [a], H.J. Kreuzer [a,*], R. Wagner [b], K. Christmann [b]

[a] *Department of Physics, Dalhousie University, Halifax, NS, Canada B3H 3J5*
[b] *Bereich Physikalische and Theoretische Chemie, Institut für Chemie der Freien Universität, Takustr. 3, D-14195 Berlin, Germany*

Received 6 March 2001; accepted for publication 13 March 2002

Abstract

A multilayer lattice gas model is set up to calculate the temperature programmed desorption spectra and other data for silver on rhenium. A careful comparison of experimental and theoretical desorption spectra implies that the surface is partially stepped with the step density likely increasing as one approaches the desorption range. Experimental temperature inhomogeneities of a few percent across the surface are suggested by careful isosteric and threshold Arrhenius analyses and theoretical modeling. A rate subtraction procedure commonly used to analyze multilayer desorption data is shown to be unnecessary. Layer plots are presented and some general features for overlapping desorption peaks are discussed.

Keywords: Non-equilibrium thermodynamics and statistical mechanics; Models of surface kinetics; Thermal desorption spectroscopy; Thermal desorption; Silver; Rhenium

1. Introduction

The study of the adsorption and multilayer growth of metals on metals by thermal desorption is still attracting considerable attention 25 years after the pioneering work of Bauer et al. [1,2]. In recent papers a study was made of silver films grown on a rhenium(0 0 0 1) surface [3]. The multipeaked temperature programmed desorption (TPD) spectra have features in common with those of Au and Cu on Mo(1 1 0), which have been modeled and analyzed successfully in a previous paper [4], but there are clear differences as well which makes this system interesting. The common leading edges of the spectra imply zero order desorption from co-existing phases in both the first and second adlayers. However, the break from the leading edge is not as sharp and the drop on the high temperature side not as sudden as for example, for Cu on Mo(1 1 0). In addition, the fact that a silver atom is slightly larger than the lattice unit cell on the Re(0 0 0 1) surface raises questions concerning lattice mismatch and incommensurability. It is argued in the experimental paper that this question can be answered by an analysis of the TPD data. When desorption peaks overlap, as occurs in this system for the peaks from the first and second (and of course all higher) adlayers, it is often suggested that a suitable subtraction should be done before an Arrhenius analysis of the data is attempted. It was shown in the previous analysis

* Corresponding author. Tel.: +1-902-494-6594; fax: +1-902-494-5191.
E-mail address: kreuzer@is.dal.ca (H.J. Kreuzer).

0039-6028/02/$ - see front matter
PII: S0039-6028(02)01696-5

of the Au/Mo(1 1 0) system that such a procedure can be misleading, and we will demonstrate this again for the present system.

A careful inspection of the TPD traces [3] for low initial coverages shows a shift of the desorption peaks to lower temperatures with increasing coverage up to about 0.2 ML, whereafter the peaks shift to higher temperatures. The initial shift to lower temperatures is unexpected for a system which must have predominantly attractive interactions to account for co-existing phases, and is absent in the data for Au and Cu on Mo(1 1 0) as just two examples. Several reasons come to mind for this shift: (i) repulsive interactions will cause a shift to lower temperatures but their range must be beyond third neighbors and with no attraction for nearer neighbors, as this would cause clustering. On the other hand, because the system exhibits coexistence beyond 0.2 ML, the lateral interactions would need to change sign. This is unreasonable from an electronic point of view. (ii) Associative desorption would also shift the desorption peaks to lower temperature. But only Ag *atoms* have been detected. (iii) A very small sticking coefficient at low coverages rising sharply at 0.2 ML would produce a shift but this is also in contradiction to experiment (and intuition) which shows that the sticking coefficient is unity at least at low temperature. (iv) Another obvious mechanism is adsorption at more strongly bound defect sites, e.g. steps, followed by adsorption onto more weakly bound terrace sites. As we will see this can easily account for the observed shift.

At low temperatures (400 K) STM images [5,6] show that the rhenium surface has terraces of varying widths, as small as 6 unit cells and as wide as 1000 cells, Fig. 6 and Figs. 2 and 3 in Ref. [6], respectively. These images also show that adsorption of silver begins at the step sites, forming clusters onto the terraces. If these step densities were maintained up to the desorption temperature their effect on desorption would be restricted to initial coverages of less than 16% and 0.1%, respectively. On the other hand, all that is needed to explain the downward shift of the TPD peaks up to 0.2 ML is some step-bunching over that part of the substrate surface from which the desorption flux was recorded. Apparently careful annealing of the surface resulted in areas of extremely large terraces, at least at low temperature, much larger than routinely achieved on other metals. Those areas were mostly sampled in the STM work. We have no direct information on whether these large terraces are maintained at desorption temperatures, or whether uneven thermal expansion of crystal and support led to step formation. Because annealed rhenium is very ductile this step formation would be reversible upon cooling. Our theoretical understanding of desorption spectra for (0 0 0 1) surfaces clearly implies that the Re substrate cannot be defect-free at desorption temperatures. Rather, the present theoretical analysis strongly suggests new and hitherto unknown physics, namely step formation at high temperatures, information that can also be extracted from TPD spectra. This does not negate the earlier STM, LEED, XPS, and TPD studies [3,5,6], which were intended to understand the growth of silver films at room temperature but suggests that additional experiments, such as LEED, preferably at desorption temperatures, should be done to verify our conclusions.

The paper is structured as follows: in the next section we outline the kinetic theory of desorption and specify the lattice gas model for a stepped surface, used for the detailed calculations. In Section 3 we present the theoretical results. We begin by showing TPD spectra for desorption from a perfect (0 0 0 1) surface and point out the discrepancies with the experimental data. This then leads us to include steps and we will see that an average step density producing terraces of 6 unit cells wide will produce spectra in which the peaks for low initial coverages do indeed shift downward in temperature appropriately. A further discrepancy between experiment and theory is the rounded break of the TPD traces from the common leading edge. We find that this discrepancy can be removed by assuming some temperature inhomogenieties across the desorption area of less than 2% of the desorption temperature. In Section 4 we present a detailed analysis of both the experimental and the theoretical TPD spectra showing in particular that a combination of isosteric and threshold analysis can be used to actually demonstrate the existence of the temperature inho-

mogeneities. In Section 5 we show that the parameters obtained allow reproduction of the TPD spectra from a highly stepped surface with an average terrace width of three adsorption sites. The last section summarizes the main points of the paper.

2. Lattice gas model

We briefly outline our theoretical approach. We model the adsorption of Ag on Re(0 0 0 1) surface by a lattice gas with hexagonal symmetry. The steps are incorporated in the lattice gas model, as developed in previous papers on adsorption and desorption on stepped surfaces [7,8], by introducing three different adsorption sites, namely on the terraces (t), on the edges of the steps (e), and at the base of the steps (b), see Fig. 1. At this stage we assume that the terrace width is uniform as it would be on a well prepared stepped surface, rather than being variable as it no doubt is on the particular Re(0 0 0 1) surface used in the experiment. We then treat the step density as a parameter and find the best (minimal) value that fits the TPD data. In addition, the lattice gas model allows for multilayer growth as developed earlier [9]. The model reduces to one for multilayer growth on a perfect step-free surface by neglecting all terms in the hamiltonian involving the step sites.

The energetics of the two-layer multi-site lattice gas model are given by a hamiltonian

$$\begin{aligned} H = & \sum_{i,j} [E_{\mathrm{t}}^{(j)} t_i^{(j)} + E_{\mathrm{b}}^{(j)} b_i^{(j)} + E_{\mathrm{e}}^{(j)} e_i^{(j)}] \\ & + \sum_j \sum_{\langle i,i' \rangle} [V_j^{(\mathrm{t-t})} t_i^{(j)} t_{i'}^{(j)} + V_j^{(\mathrm{t-b})} t_i^{(j)} b_{i'}^{(j)} \\ & + V_j^{(\mathrm{t-e})} t_i^{(j)} e_{i'}^{(j)} + V_j^{(\mathrm{b-e})} b_i^{(j)} e_{i'}^{(j)}] \\ & + \sum_{\langle i,i' \rangle} [V_{1,2}^{(\mathrm{t-t})} t_i^{(1)} t_{i'}^{(2)} + V_{1,2}^{(\mathrm{b-e})} e_i^{(1)} b_{i'}^{(2)}] + \cdots \end{aligned} \tag{1}$$

Here i, i' labels the adsorption sites and $j = 1, 2$ the first and second layers. The occupation numbers $t_i^{(j)}$, $b_i^{(j)}$ and $e_i^{(j)}$ are zero or one, depending on whether the terrace, base or edge sites i in layer j are empty or occupied. The single particle free energies are given, here for the terrace sites, by

$$E_{\mathrm{t}}^{(j)} = -V_{\mathrm{t}}^{(j)} - k_{\mathrm{B}} T \ln(q_{3t}^{(j)}) \tag{2}$$

where $V_{\mathrm{t}}^{(j)}$ is the positive binding energy of a single silver atom to rhenium for $j = 1$ and to a silver atom in the first layer for $j = 2$. Likewise, $q_{3t}^{(j)}$ are the single particle partition functions accounting for the vibrations of a silver atom perpendicular and parallel to the surface; they are approximated by a product of three harmonic oscillators with frequencies (here for the terrace sites) $\nu_{\mathrm{tx}}^{(j)}$, $\nu_{\mathrm{ty}}^{(j)}$, and $\nu_{\mathrm{tz}}^{(j)}$, different in the first and second layers and for the different adsorption sites, generally. We restrict the intra and interlayer lateral interactions to be to nearest and some next-nearest neighbors, which is sufficient for systems with mainly attractive interactions, e.g. $V_j^{(\mathrm{t-t})}$, $V_j^{(\mathrm{t-b})}$ are intralayer interactions between Ag atoms on neighboring terrace sites and between a terrace and a base site. Similarly $V_j^{(\mathrm{b-e})}$ is a next nearest neighbor interaction across a step; however, we omit interactions of longer range parallel to the step edges. $V_{1,2}^{(\mathrm{t-t})}$ and others are interactions between Ag atoms on neighboring sites in the two layers; interlayer interactions between silver atoms in ontop positions are included in $V_\alpha^{(2)}$ for $\alpha = \mathrm{t}, \mathrm{b}, \mathrm{e}$.

To describe the adsorption and desorption kinetics we make use of the fact that, in the temperature range of desorption, surface diffusion is so fast on the time scale of desorption that quasi-equilibrium is maintained in the remaining adsorbate. That is to say, as particles desorb the remaining adsorbate redistributes itself so that the distribution among the various sites and layers and

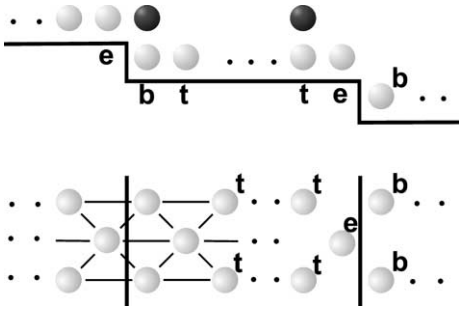

Fig. 1. Side and top views of edge (e), base (b) and terrace (t) sites of the lattice gas model. Black discs represent second layer adatoms; fine lines indicate lateral interactions.

all correlation functions are those of equilibrium at the instantaneous temperature and the remaining coverage. Under such conditions (of quasi-equilibrium) the adsorbate is completely described by the partial coverages, e.g. for the $N_t^{(j)}$ terrace sites in layer $j = 1, 2$

$$\theta_t^{(j)} = \frac{1}{N_t^{(j)}} \sum_i \left\langle t_i^{(j)} \right\rangle \tag{3}$$

These partial coverages are subject to kinetic equations [9,10]

$$\frac{d\theta_t^{(j)}}{dt} = S_t^{(j)}(\theta, T) \frac{a_t \lambda_{th}}{h} P - S_t^{(j)}(\theta, T) \frac{a_t}{\lambda_{th}^2 q_{3t}^{(j)}} \times \frac{k_B T}{h} e^{-V_t^{(j)}/k_B T} \frac{\theta_t^{(j)}}{1 - \theta^{(j)}} e^{\mu_a^{(int)}/k_B T} \tag{4}$$

with similar equations for the partial coverages of the base and edge sites. Here a_t is the area of a terrace adsorption site, $\lambda_{th} = h/\sqrt{2\pi m k_B T}$ is the thermal wavelength of a silver atom of mass m, P is the pressure of the gas phase above the surface, and

$$\theta^{(j)} = \theta_t^{(j)} + \theta_e^{(j)} + \theta_b^{(j)} \tag{5}$$

is the coverage in the jth layer. $\mu_a^{(int)}$ is the part of the chemical potential of the adsorbate accounting for the energetic differences in the various sites and layers and also for all lateral interactions ($\mu_a^{(int)} = 0$ for a homogeneous surface and in the absence of lateral interactions); its dependence on temperature and coverage will be calculated on the basis of the hamiltonian (1) employing the transfer matrix method, a standard procedure of statistical mechanics and our preferred choice [10].

The sticking coefficients, $S_t^{(j)}$, etc. are a measure for the efficiency of energy transfer in adsorption, and thus are temperature and coverage dependent. Since energy supply from the substrate is required for desorption, the sticking coefficient, albeit usually at a higher temperature, must appear in the desorption rate by the detailed balance argument. The sticking coefficient cannot be obtained from thermodynamic arguments but must be calculated from a microscopic or mesoscopic theory or be postulated in a phenomenological approach, based on experimental evidence for a particular system or some simple arguments. For silver on Re(0 0 0 1) we can safely assume that all sticking coefficients are constant and unity.

3. Theoretical results

To study the particular effects of steps on TPD spectra we first present the closest possible fit to the data with a model that assumes a perfectly flat Re(0 0 0 1) surface. To this end we drop all terms in the hamiltonian (1) except those that refer to the terrace sites. We recall that the binding energies with which a single Ag atom binds to the surface or to the first Ag layer, $V_t^{(1)}$ and $V_t^{(2)}$, respectively, control the peak positions of the desorption spectra at low coverages. The adatom vibrational frequencies, $\nu_{tx}^{(j)}$, $\nu_{ty}^{(j)}$, and $\nu_{tz}^{(j)}$, entering via the partition functions in (2), control the widths of the peaks, and the lateral attractions, $V_1^{(t-t)}$ and $V_2^{(t-t)}$, are reflected in the slope of the common leading edges of the first and second layer spectra, respectively. In principle these parameters could be obtained from ab initio calculations [11] or taken over from other, independent measurements such as vibrational spectroscopy or from the analysis of equilibrium data. Neither is available for the present system and we adjust these parameters to obtain the best possible fit to the experimental data. With reasonable choices of these parameters, we first calculate the chemical potential which appears in (4), using the transfer matrix method, and compute the desorption spectra [12]. The best fit thus obtained is shown in Fig. 2 for initial coverages up to 1 ML. Although the common leading edge of the experimental spectra is reproduced quite well [3], several features make this fit unacceptable: (i) the break of the traces from the leading edge is too sharp, and shifts uniformly to higher temperatures with increasing initial coverage (i.e. the observed downward shift in the peak positions for low initial coverages is absent); (ii) the theoretical spectra are too narrow; and (iii) the trailing edge drops much too abruptly. We could improve the fit by reducing the nearest-neighbor attraction and smearing the spectra over a temperature interval of 25 K, say, which would mimick temperature inhomogeneities during the desorption process. Although the weaker attraction spreads out the leading edge,

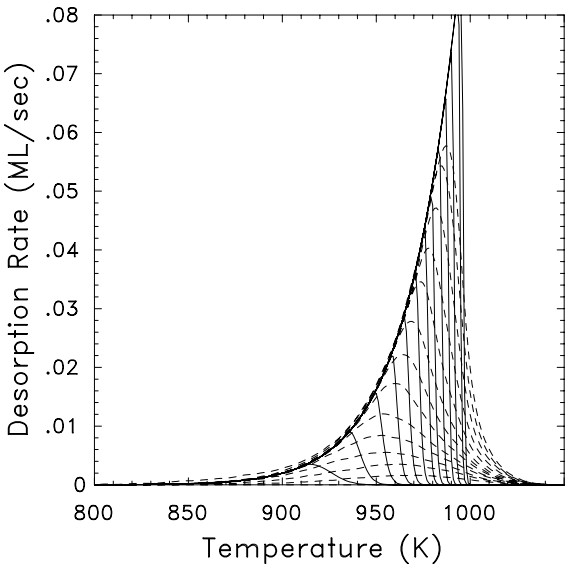

Fig. 2. TPD spectra for Ag/Re(0 0 0 1) with a heating rate of 2.5 K/s. Dashed lines: experimental data for initial coverages $\theta_0 = 0.052$, 0.11, 0.18, 0.25, 0.32, 0.40, 0.48, 0.55, 0.64, 0.73, 0.82, 0.93, 1.00 ML. Solid curves: theoretical model, for the first monolayer on an atomically flat surface, with parameters: binding energy $V_t^{(1)} = 275$ kJ/mol, vibrational frequencies $\nu_t^{(1)} = 6.0 \times 10^{12}$ s^{-1}; lateral interaction $V_1^{(t-t)} = -10.8$ kJ/mol.

because desorption would then proceed above the critical temperature, the breaks from the common leading edge and the widths of the traces would approximate the experimental curves better. However, this does not introduce a downward shift of the peaks of the low initial coverage traces. This can only be achieved by introducing steps, as we will do next.

To account for the shift of the experimental peaks in Fig. 2 of Ref. [3] to lower temperatures for increasing initial coverages up to about 0.2 ML we assume, as discussed in Section 1, that this is due to the initial occupation of defect sites, i.e. steps, followed by adsorption onto more weakly bound terrace sites. This implies a terrace width of about 6–8 rows of adsorption sites. Then to obtain a good fit for coverages below 0.2 ML we adjust the parameters in the site free energies, $E_t^{(1)}$, $E_b^{(1)}$ and $E_e^{(1)}$, involving both binding energies and vibrational frequencies. The parameters for the step sites we obtain by fitting to the peak positions and the widths of the lowest coverage TPD curves. From STM studies [6] we know that the base sites are more strongly bound and we find a binding difference to the terrace sites of about 48 kJ/mol; to keep the number of adjustable parameters to a minimum we assume $E_t^{(1)} = E_e^{(1)}$ and equal vibrational frequencies for all sites. Next, because of the common leading edge in the TPD spectra, we expect that the lateral interactions are attractive and adjust their strengths to get a good fit up to monolayer coverage. Again for simplicity, we assume first neighbor interactions only (generally a good assumption for systems with attractive lateral interactions) and take them the same between all nearest neighbors on the terraces, but different between neighboring edge and base atoms across the steps. We find $V_1^{(\alpha-\beta)} = -12$ kJ/mol (α, β = t, e, b) except $V_1^{(b-e)} = -17$ kJ/mol. The overall result for the first monolayer is in good agreement with experiment, Fig. 3. The fact that the leading edge

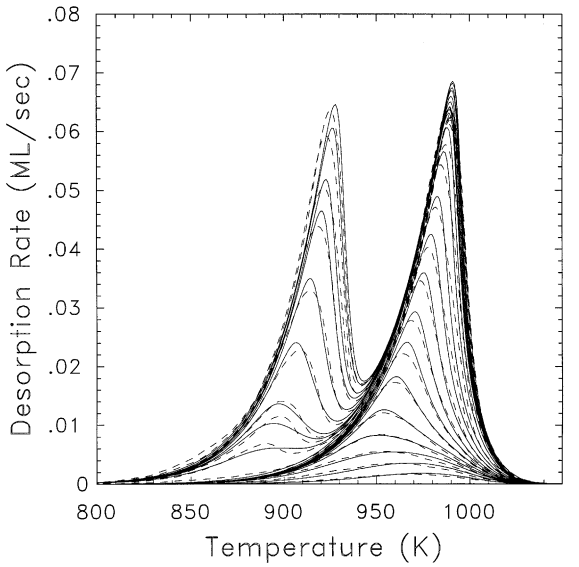

Fig. 3. TPD spectra for Ag/Re(0 0 0 1) with a heating rate of 2.5 K/s. Dashed lines: experimental data for initial coverages $\theta_0 = 0.052$, 0.11, 0.18, 0.25, 0.32, 0.40, 0.48, 0.55, 0.64, 0.73, 0.82, 0.93, 1.00, 1.14, 1.22, 1.27, 1.41, 1.55, 1.70, 1.77, 1.89, 1.95 ML. Solid curves: theoretical model with parameters: first silver layer binding energies $V_t^{(1)} = V_e^{(1)} = 268$ kJ/mol, $V_b^{(1)} = 316$ kJ/mol; second layer binding energies $V_t^{(2)} = V_e^{(2)} = 206$ kJ/mol, $V_b^{(2)} = 254$ kJ/mol, vibrational frequencies $\nu_\alpha^{(j)} = 6.0 \times 10^{12}$ s^{-1} for $j = 1$, 2 and α = t, b, e; lateral interactions $V_1^{(\alpha-\beta)} = -12.2$ kJ/mol, $V_2^{(\alpha-\beta)} = -10.8$ kJ/mol, $V_{1,2}^{(e-b)} = -17.5$ kJ/mol.

in the theory is not as well-defined as in the experiment has no physical basis but is simply due to the fact that in our implementation of the transfer matrix method we were restricted by computer memory to use a finite strip width [10]. We have checked the dependence of the fit on the width of the terraces; a 6-row terrace gives the best fit.

Looking at the spectra for initial coverages between 1 and 2 ML we repeat this procedure to get the parameters for the second layer, keeping the vibrational frequencies the same as in the first monolayer but adjusting binding energies and lateral interactions. Again, for coverages just above a monolayer the peak positions of the experimental traces appear at higher temperatures relative to the leading edge of the second layer, than would be seen on a homogeneous surface. We attribute this to the second layer also forming at the base sites first. This is due to the fact that a second layer atom at a base site is not only bound more strongly to the first layer than one of its second layer terrace neighbors but also (for equal lateral interactions between second layer atoms) interacts attractively with two nearest neighbor first layer edge atoms (in the completed monolayer) of an adjacent terrace. Again, to keep the number of parameters at a minimum we impose identical binding energy differences between first and second layer sites, $V_{\alpha}^{(1)} - V_{\alpha}^{(2)} = 62$ kJ/mol. We find similar intralayer interactions for the second layer as for the first, $V_2^{(\alpha-\beta)} = -11$ kJ/mol (α, β = t, e, b). For the additional attraction between the second layer base and first layer edge atoms we get $V_{1,2}^{(\mathrm{b-e})} = -17$ kJ/mol for the best fit.

In Fig. 3 we show a satisfactory fit to the experimental data with the corresponding parameters listed in the figure caption. As a general feature the theoretical spectra are slightly higher at the peaks and consequently narrower than the experimental data. We will discuss this small discrepancy below. There is always some ambiguity in defining the completion of a monolayer in the TPD spectra in the absence of other experiments. In the previous experimental paper, a monolayer was inferred from the positions of the rate minima in the layer plots. However, this inference is suspect as we discuss below. Instead we have chosen to use the last trace without an inflection point (that would signal the onset of the second layer). To obtain the theoretical fit to the experimental data we therefore renormalized the rates and find that the initial coverages are slightly lower, by a factor 0.95 than those previously published and within the tolerance of the experiment.

To understand the kinetics of this system we have extracted, from the theory, the partial desorption rates from the first and second layer and also from the various adsorption sites. As the partial rates from the first and second layer, Fig. 4(a), clearly indicate, desorption, and thus adsorption, is layer by layer. Looking first at desorption from a full monolayer we find that it starts at the temperatures at which the second layer itself desorbs. However, as the initial coverage is increased above a monolayer the partial desorption rate from the first layer, $-\mathrm{d}\theta^{(1)}/\mathrm{d}t$, is suppressed up to temperatures where the second monolayer has almost completely disappeared. And this onset of first layer desorption is to higher temperature with higher initial coverage. This fact has a very important consequence for the analysis of TPD spectra for initial coverages larger than 1 ML, namely, it is inappropriate to subtract the TPD spectrum for initial coverage of 1 ML from the spectra with higher initial coverages to obtain the TPD spectra of the second layer alone. This is discussed further below.

Partial desorption rates from the three types of sites (α = t, b, e) in both layers, $-\mathrm{d}\theta_{\alpha}^{(j)}/\mathrm{d}t$, are shown in Fig. 4(b). Looking first at initial coverages below a monolayer, we see that the interior terrace sites empty out first followed by those terrace and edge sites which are adjacent to the strongly bound base sites, which remain occupied to the highest temperatures. A similar situation pertains for initial coverages larger than a monolayer.

The growth modes can be followed in detail in the (equilibrium) partial site coverage plots, $\theta_{\alpha}^{(j)}(\theta)$, in Fig. 4(c). Starting at the lowest coverages the base sites fill first up to a coverage of about 1/6 ML, at which stage edge sites and also terrace sites start to be occupied because their attraction to the base sites compensates for their lower binding energies. This repeats when the second layer fills up, and for both layers more mixing of site occu-

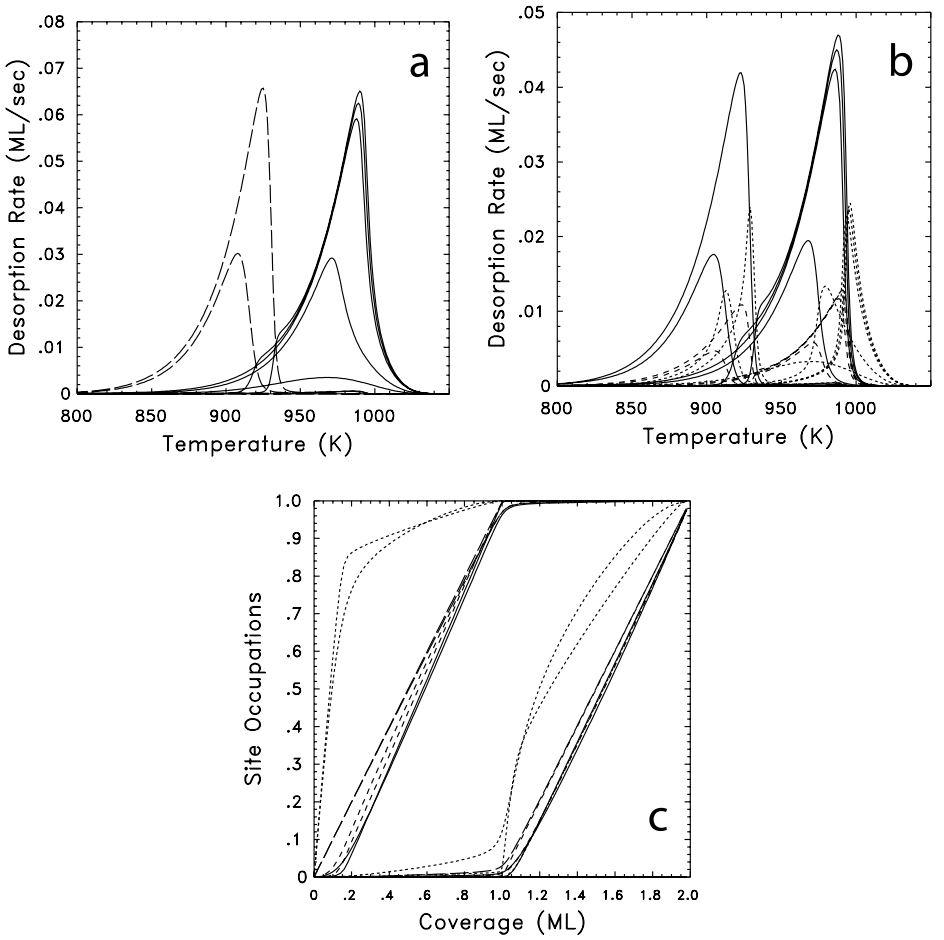

Fig. 4. (a) Model partial desorption rates from the first (solid lines) and second (dashed lines) layers for initial coverages $\theta_0 = 0.11$, 0.55, 1.0, 1.46, 1.95 ML. (b) Individual site contributions, $-\mathrm{d}\theta_\alpha^{(j)}/\mathrm{d}t$ to these rates: base sites ($\alpha = \mathrm{b}$)—dotted lines, terrace sites ($\alpha = \mathrm{t}$)—solid lines, edge sites ($\alpha = \mathrm{e}$)—dashed lines. (c) Equilibrium layer partial coverages, $\theta^{(j)}(\theta)$, Eq. (5) (long-dashed lines) for two temperatures spanning the desorption range $T = 700$, 1000 K; and corresponding site occupations $\langle \alpha_i^{(j)} \rangle$ for $\alpha = \mathrm{t}$, b, e with line types as above. $T = 700$ K curves exhibit the sharpest features.

pations occurs at higher temperatures. Despite this non-uniform filling of the three types of sites, the partial coverages in the first and second layers rise linearly with coverage such that $\theta^{(1)} = \theta$ for $\theta < 1$ and $\theta^{(2)} = (\theta - 1)$ for $\theta > 1$.

The next point we want to make concerns the layer plots. Both the theoretical and the experimental spectra, Fig. 5, show a shift of the minima at about monolayer initial coverage to lower coverages. The abrupt change in the respective shifts of the minima positions near the completed monolayer has been interpreted as the signature of the fact that silver atoms are too large to fit into the Re(0 0 0 1) lattice structure. Thus for coverages larger than 1 ML the silver lattice should expand leading to a reduction in the maximum coverage possible as emphasized in the earlier work [3]. Because our theory does not include lattice relaxation it is unable to reproduce the specific dependence of these rate minima. Nevertheless, we want to point out in addition that the shifts in the minima of layer plots themselves need not arise from lattice mismatch: In our theory there is no such mismatch, yet the theoretical spectra exhibit

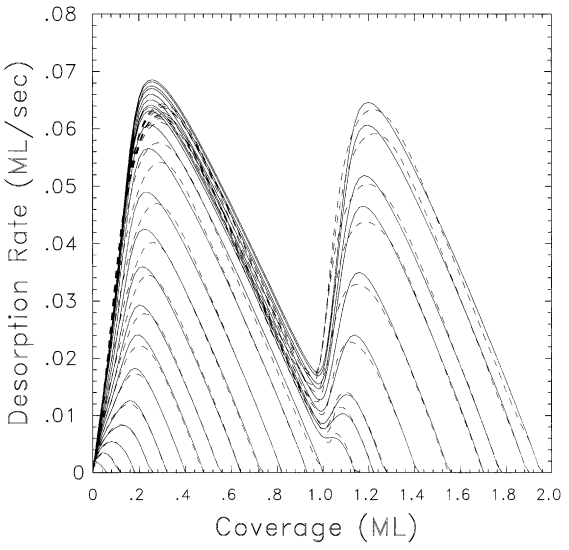

Fig. 5. Layer plots of the desorption rates of Fig. 3 vs. instantaneous coverage.

the same trend in moving the minimum to smaller coverages, as observed in the experimental layer plots. This results simply from the fact that the first and second layer peaks overlap. Indeed, if we artificially reduce the gap between the two peaks (by raising the binding energy of Ag in the second layer) we can increase the shift in the interlayer minimum by up to 10%. This shift also has nothing to do with the fact that there are attractive interactions between adsorbed silver atoms. Reducing the lateral interactions to zero, or even making them repulsive (which changes the shape of the two desorption peaks considerably removing the leading edge altogether) does not affect the qualitative picture of the shift of the minimum. On the other hand the shift disappears as the second layer peak is separated from that of the first layer.

4. Analysis of spectra

Having obtained good agreement of the theoretical TPD spectra with the experimental data, we can infer additional information about the system from a proper Arrhenius analysis of both sets of spectra. Such an analysis does not replace and is not a theory but a mere parametrization. The purpose is to reduce the multitude of TPD traces for different initial coverage to just two coverage dependent functions, namely the desorption energy and the effective prefactor, obtained by parametrizing the desorption rate as

$$\frac{\mathrm{d}\theta}{\mathrm{d}t} = -\nu_{\mathrm{eff}}(\theta)\mathrm{e}^{-E_{\mathrm{d}}(\theta)/k_{\mathrm{B}}T} \tag{6}$$

Such an analysis, for TPD data obtained by variation of initial coverages, can be performed using the isosteric [13,14] or threshold [15] method. For 'perfect' data (i.e. without systematic or statistical errors, such as calculated spectra) these two analyses (and the method of heating rate variations) give identical results. [1] For the theoretical spectra in Fig. 3 the resulting desorption energy and prefactor are shown in Fig. 6 (solid lines). At zero coverage the desorption energy is, to within vibrational contributions, the binding energy of the base sites. With increasing coverage $E_{\mathrm{d}}(\theta)$ reflects firstly the effective lowering of the binding energy in the first layer as the weaker bound edge and terrace sites become occupied. This trend is reversed above $1/6$ ML as a result of the lateral attraction. At the completion of a monolayer, $E_{\mathrm{d}}(\theta)$ drops suddenly by an amount roughly equal to the binding difference for first and second layers. Because for a system in quasi-equilibrium the desorption energy (plus $k_{\mathrm{B}}T/2$) is the isosteric heat of adsorption (in the absence of precursors) we expect the desorption energy from the second layer to be greater than the cohesive energy of the bulk metal (274 kJ/mol for silver).

The lateral attractions, deduced from fitting the leading edges of the experimental spectra, are such that for a homogeneous substrate [4] the temperature range of desorption is below the critical temperature for the coexistence of dilute and condensed phases, $T_{\mathrm{c}} \simeq -1.1V^{(\mathrm{t\text{–}t})}$ for a hexagonal lattice. As shown in Fig. 2, this leads to sharp leading edges in the TPD spectra, typical of zero order desorption, and to a corresponding coverage-independent desorption energy plateau over

[1] All Arrhenius analyses, both for the experimental and the theoretical TPD spectra, have been done with the ASTEK program, see [12].

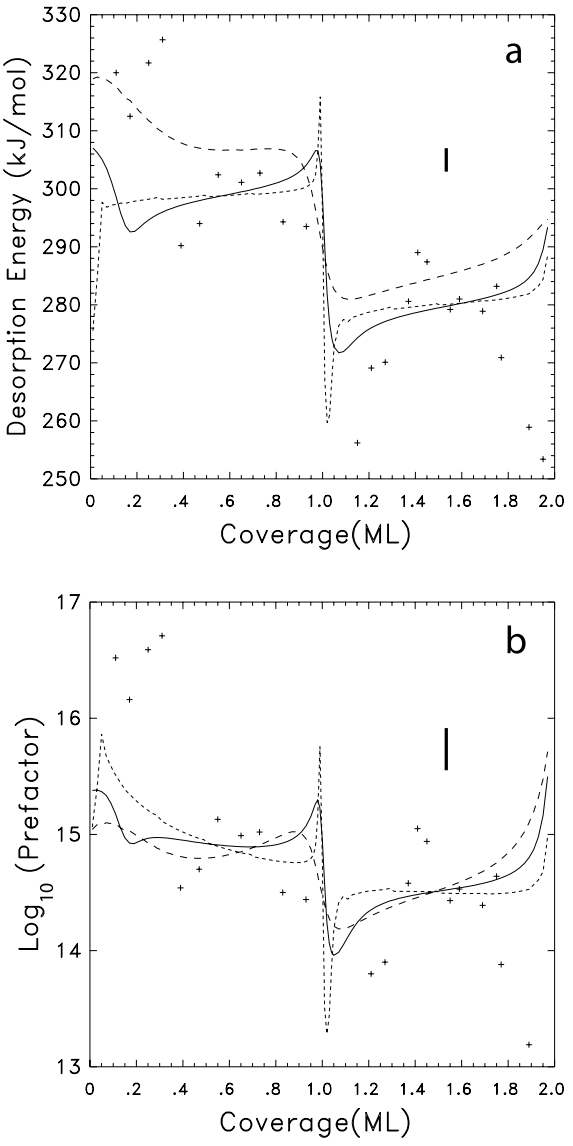

Fig. 6. (a) Desorption energy, from an Arrhenius analysis of experimental and theoretical TPD spectra: solid line—analysis of theoretical curves in Fig. 3; dotted line—analysis of model spectra for a homogeneous Re substrate, spectra of Fig. 2; crosses—from a threshold analysis of the experimental spectra of Fig. 3. (The vertical bar is an estimate of the error inferred by changing the initial depletion in the analysis.) Dashed line—analysis of theoretical curves in Fig. 10. (b) Corresponding prefactors from Eq. (6), $\nu_{\mathrm{eff}}(\theta)/\theta$.

the coexistence region (away from zero and full monolayers), after an initial rise in the low coverage (dilute) regime from the single particle binding energy, V_{t}, to $V_{\mathrm{t}} - 3V^{(\mathrm{t-t})}$. This is shown in Fig. 6(a) as a dotted line. That we see a rise around $1/2$ and $3/2$ ML for the full model with steps is largely due to our computational limitation discussed earlier. The prefactor in Fig. 6(b) shows a coverage dependence in accordance with zero order desorption.

We have also re-analyzed the experimental data performing both an isosteric and a threshold Arrhenius analysis using the ASTEK software package [12]. The results for the threshold analysis have been included in Fig. 6 and with an estimate of our error resulting from the choice of fractional depletion used in the analysis. We should also point out that the threshold analysis is sensitive to the background subtraction. Overall magnitudes of desorption energy and prefactor are in good agreement with the theoretical values and qualitative features such as the rise below about 0.2 ML and the drop at 1 ML are in common.

The results of this threshold analysis of the experimental TPD spectra are in some disagreement with those obtained in the previous work [6] using the isosteric analysis (we repeat again that for 'perfect' data these two procedures should yield the same result). We have therefore repeated the isosteric analysis, Fig. 7 (crosses). Similar values of desorption energy and prefactor to Fig. 6 (crosses) are found in the mid-coverage range of the first monolayer, but a decrease below 0.3 ML (where it should rise to reflect the binding to the stronger base sites). The difference in the desorption energy between the mid-coverage regime of the first and second layer, respectively, is only half of what the threshold analysis gives, and what we need in the theory to fit the peak separation.

Next we illustrate the inadmissability of subtracting the monolayer desorption trace from the higher initial coverage spectra. As we discussed above for overlapping first and second layers there is a delay in the onset of desorption from the first layer to higher temperatures for initial coverages larger than a monolayer. This implies, among other things, that the remaining first layer peak gets modified, most noticeably in the trailing edge. We can see this clearly in both the experimental and theoretical spectra when we subtract the

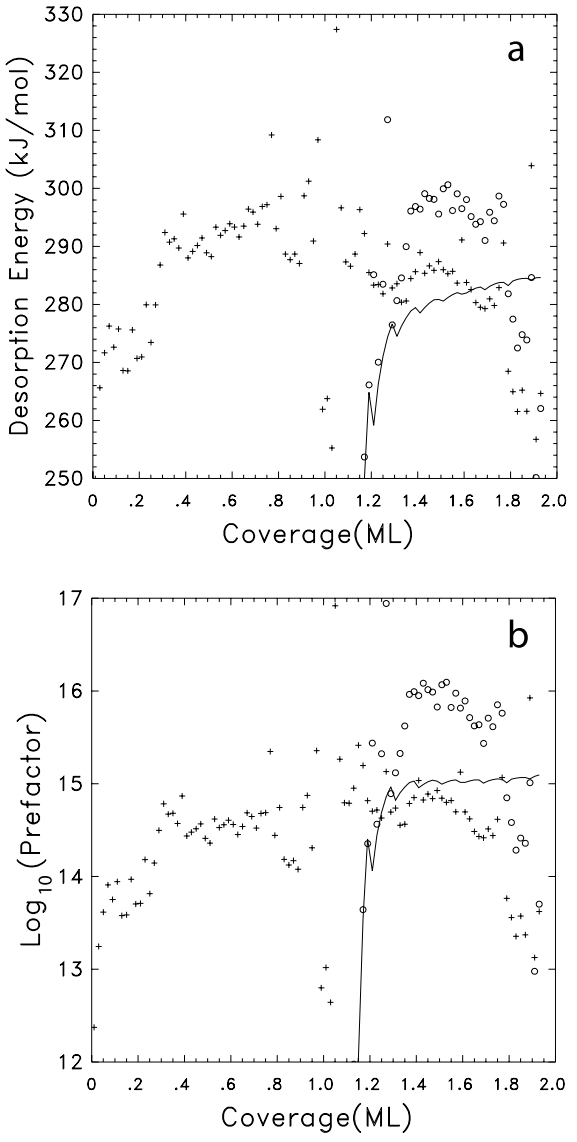

Fig. 7. Desorption energies (a) and prefactors (b) from an isosteric analysis of the experimental data. Crosses: analysis of the complete set of spectra up to 2 ML, dashed lines in Fig. 3. Circles: analysis of the second layer after subtraction of the 1 ML rate curve, see Fig. 8(b). Solid line: corresponding results for such a subtraction of the model spectra, see Fig. 8(a).

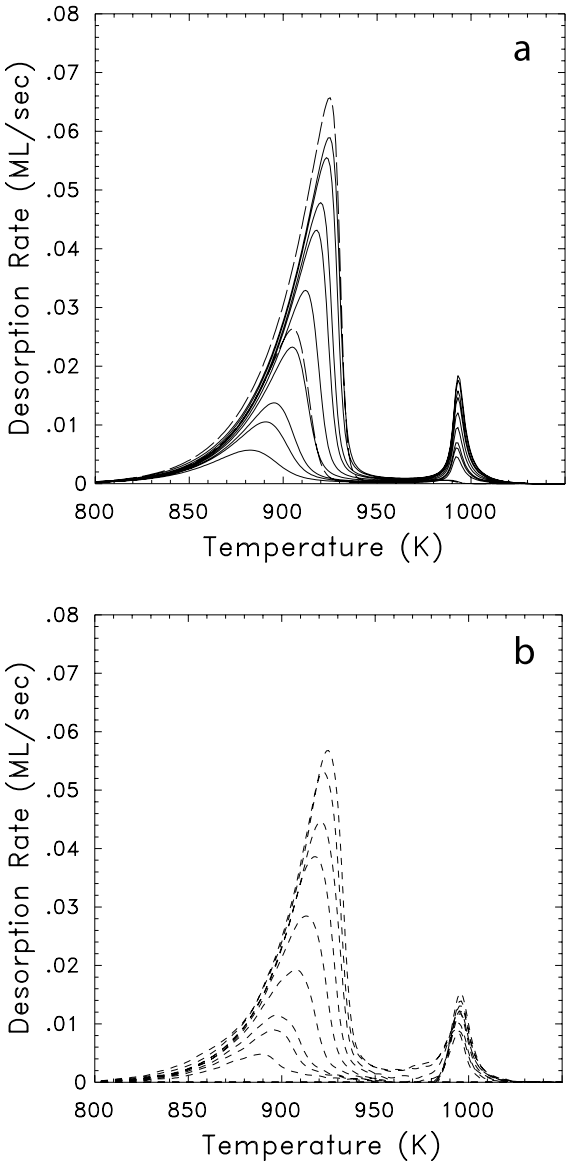

Fig. 8. TPD rates obtained by subtracting the monolayer rate from all higher initial coverage curves in Fig. 3, for model (a) and experimental spectra (b) of Fig. 3. Dashed lines in (a) are partial desorption rates from the second layer for $\theta_0 = 1.41$ and 1.95 ML.

$\theta_0 = 1$ desorption trace from those with larger θ_0, see Fig. 8, where this modification leads to a residual peak at the position of the submonolayer spectra, as discussed above in connection with the layer partial rates and also in previous work [4]. For comparison we also show in Fig. 8(a) the actual second layer partial rates for two initial coverages (cf. Fig. 4(a)). The subtracted rates are less throughout the range of the second layer desorption because of the erroneous subtraction of the

$\theta_0 = 1$ rate which starts well below the second layer peak. The difference appears in the residual peak at higher temperatures, and arises simply from the overlap of the first and second layer peaks. Indeed, if we artificially reduce the gap between the two peaks (by raising the binding energy of Ag in the second layer) we can increase the residual peak.

A threshold analysis of these (subtracted) spectra yields results close to those of the unsubtracted spectra for all θ_0, because the initial rates (at the lowest temperatures) are least effected by the subtraction. However, an isosteric analysis produces different results in the low coverage regime of the second layer due to the existence of the residual peak around 1000 K. This is shown in Fig. 7 as a drop below about 1.4 ML. For completeness we also show the results of an isosteric analysis of the subtracted experimental second layer spectra (Fig. 8(b)) in Fig. 7 (circles). The latter results differ from those of the analysis of the unsubtracted experimental spectra and also from the model data. There are a number of reasons for this such as our different normalization of the initial coverages, and the overall subtraction of a background from all experimental desorption traces.

We will now show that the qualitative difference in the desorption energy and prefactor between the results from the threshold and isosteric analyses of the experimental data, at low (submonolayer) coverage, may be due to deviations in the temperature ramp from a perfectly linear and constant heating rate and/or inhomogeneities in the temperature across the sample surface. Whether this is the case for the present data is not certain without further experiments. However, it is worth pointing this effect out because it stipulates high quality temperature control in TPD experiments. To show this we have averaged the theoretical rates over a small temperature range of 10 K, i.e. assuming an inhomogeneity of the temperature across the sample of about 1%. In light of the experimental difficulties in controling and measuring temperatures around 1000 K this inhomogeneity is an expected lower bound. The effect on the spectra themselves is that the peaks get broadened and lowered with the trailing edge less precipitous, the more so the sharper the peaks. The latter fact has the immediate consequence in the isosteric Arrhenius analysis of lowering the desorption energies and prefactors at low coverages, solid line in Fig. 9. Most importantly, the isosteric Arrhenius analysis of these smeared (theoretical) data show

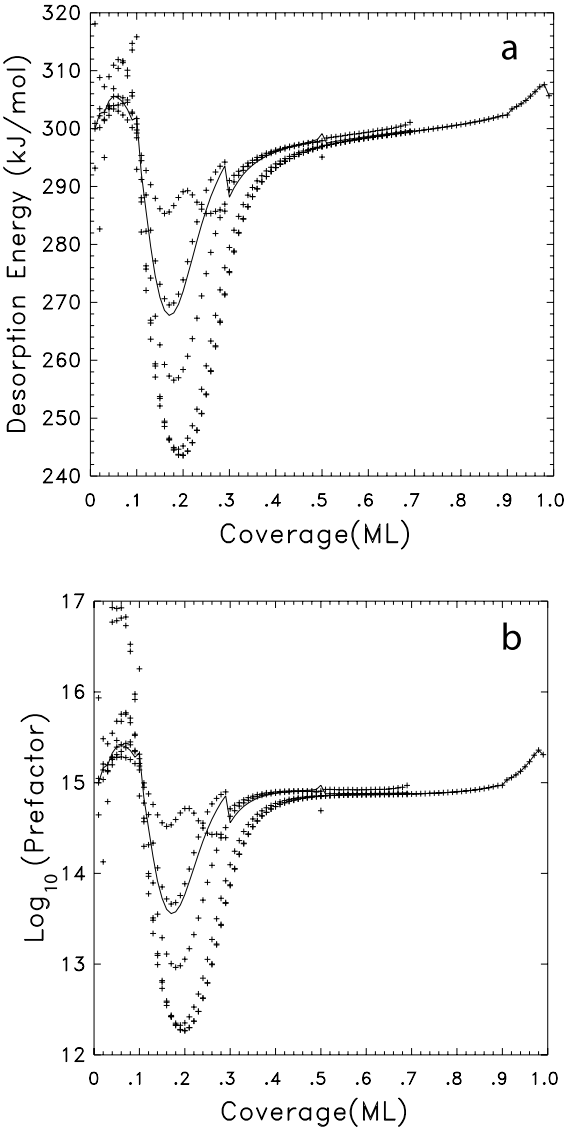

Fig. 9. Desorption energies (a) and prefactors (b) from an isosteric analysis of model rates, averaged over a range of 10 K to account for temperature inhomogeneities, for $\theta_0 = 0.1$, 0.3, 0.5, 0.7, 0.9, 1.0 ML in steps of 0.1 ML. Solid line is a linear fit to the (curved) isosteric rates (as a function of $1/T$). Crosses: local slopes of these isosteres.

the same low coverage behaviour of the desorption energy and prefactor as the isosteric analysis of the experimental data. Averaging over a larger temperature window will enhance the drop even further. Temperature inhomogeneities can be viewed as a non-equilibrium effect and as such will result in isosteric rates which are patently not linear in $1/T$. This can be illustrated by plotting the differential desorption energy, i.e. the local slope of the Arrhenius plots [16]. This varies for different initial coverages as shown in Fig. 9: the solid line is simply the straight line approximation to the (curved) isosteres. The latter is qualitatively similar to the experimental data. (The discontinuities in Fig. 9 are not due to an error in the analysis but occur as the chosen isosteres cross the initial coverages of the TPD spectra. In this case two adjacent isosteres sample the desorption rates at considerably different temperatures. Such effects are rarely seen in experimental data where they are averaged out by the noise in the rates.) In any case, temperature inhomogeneities are a likely explanation why so many (isosteric) analyses of experimental data show a precipitous drop in both desorption energy and prefactor for low coverages where in addition all experimental uncertainties have accumulated. Effects of temperature inhomogeneities on TPD spectra have been discussed also by Carter and Anton [17].

There is a straightforward check to lend further credence to our hypothesis and that is to perform a threshold analysis on the TPD data. In this case we only take the data over a small depletion of the initial coverage, and the effect of temperature inhomogeneities can be reduced substantially. Indeed, performing a threshold analysis of the temperature smeared theoretical spectra we recover completely the results of the analysis of the unsmeared data including the rise of the desorption energy (reflecting the larger binding at the steps) and prefactor towards zero coverage.

5. Desorption from a surface with high step density

We recall that in our attempt to model an important detail in the low initial coverage TPD spectra, namely the shift of the desorption peaks to lower temperatures, we invoked a step density of six adsorption sites per terrace. To shed further light on this problem we have performed TPD experiments from a surface with a high step density with terrace widths of about three adsorption sites. If our theory is correct we should expect a fit to these data, without changing any parameters except the terrace width. Indeed, this is the case as will be shown in more detail in a forthcoming work. One qualitative difference between the experimental submonolayer spectra obtained from the smooth and the high step density rhenium surfaces, compare the dashed lines in Figs. 3 and 10, is the disappearance of the common leading edge. This is simply the consequence of the size effect [7,8] associated with small systems in which phase transitions are suppressed. There is also a difference in the widths and positions of the TPD peaks in the submonolayer regime.

If we retain all the parameters of the fit to the data of Fig. 3 we can reproduce the gross features

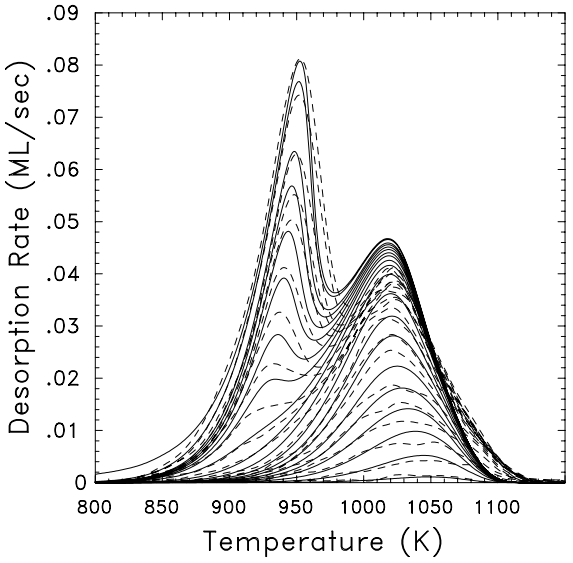

Fig. 10. TPD spectra for Ag desorbing from a high step density Re surface with a heating rate of 4.1 K/s. Experimental data (dashed lines) for initial coverages $\theta_0 = 0.02$, 0.1, 0.18, 0.26, 0.37, 0.44, 0.56, 0.66, 0.74, 0.80, 0.88, 0.97, 1.10, 1.18, 1.35, 1.45, 1.56, 1.59, 1.88, 2.0 ML. Theoretical model (solid lines) with parameters of Fig. 3, except for terrace width of three sites instead of six. Only binding energies and lateral interactions of Fig. 3 have been changed, respectively, by +5% and −20%.

of the TPD data from the high step density surface. The minimal changes needed to get a fit, solid lines in Fig. 10, is an increase in the binding energies to the surface by 5%, and a decrease in the lateral attraction by about 20%, keeping the difference in binding energies between step and terrace sites the same. These changes are reflected in the desorption energy, obtained by an Arrhenius analysis of the model data, in Fig. 6a. This is easily understood when one considers that this surface with a high step density is closer to an open surface if the steps were arranged in a regular pattern. Such open surfaces typically have a larger electronic density in the surface region which can be used by the adatoms for stronger binding to the surface, thus reducing concomitantly the availability of electrons for lateral binding. A complete analysis and modeling of this system together with that of desorption of Cu from the same surface, will be given elsewhere.

6. Summary

In this paper we have set up a lattice gas model for the adsorption of silver on Re(0 0 0 1) up to 2 ML. Careful inspection and analysis of the experimental TPD data resulted in the following details of the model:

(1) The leading edge of the TPD spectra in both the first and second layers indicate attractive lateral interactions strong enough to maintain the adsorbate below its critical temperature throughout the desorption range.

(2) The substantial shifts of the TPD peaks to lower temperatures for initial coverages below about 0.2 ML suggest the presence of more strongly bound adsorption sites. These have been incorporated in the lattice gas model as step sites in addition to (the more weakly bound) terrace sites.

Fitting the model to the experimental TPD data allowed us to estimate the parameters of the lattice gas such as the binding energies of silver atoms at terrace and step sites in the first and second layers, their vibrational frequencies with respect to the surface, and their lateral attractive interactions.

Although the model produced a satisfactory fit to the TPD data, we explored possible origins of small but systematic deviations by re-analyzing the experimental data, performing Arrhenius analyses to extract desorption energies and prefactors which we then compared to those obtained from the theoretical spectra. We employed both the threshold and the isosteric methods. These give identical results for 'perfect' data such as the theoretical spectra but for 'real' data, which always have error bars associated with them, the threshold analysis is more accurate, even for 'good' data as that analyzed here. The reason is that any inhomogeneities in temperature, either due to small instabilities in the heating rate or due to uneven heating of the substrate, have a cumulative effect on TPD spectra so that the high temperature/low coverage part is the most affected. This, we showed, results in a substantial drop in both desorption energy and prefactor towards low coverage when the isosteric method is used, whereas a threshold analysis produces a rise reflecting the (true) stronger binding at the base sites.

To simulate these temperature inhomogeneities we smeared the theoretical TPD data over a range of 10 K, or 1% of the desorption temperature and recovered the trends exhibited by the analyses of the experimental data. Again, this suggests that it is mandatory to do both threshold and isosteric analyses to extract the maximum amount of information from TPD data: Although the threshold analysis gives a more accurate picture of the energetics of the adsorbate, the isosteric analysis gives information, among others, on possible temperature inhomogeneities. Non-equilibrium effects, such as these, will result in curved isosteres in the Arrhenius plots which advantageously are analyzed using the differential desorption energies along the isostere instead of a linear approximation.

Our last point concerns the practice in the analysis of multipeak desorption peaks of extracting single peak spectra by some subtraction procedure. As we show in detail this procedure is incorrect; and unnecessary because the analysis of the complete set of spectra can be done without impunity, in particular employing the threshold method.

What we hope to have shown in this paper is that the combination of theoretical modeling of the experiment together with a complete analysis of both experimental and theoretical 'data' yields the maximum information about a system and puts any interpretation on firmer grounds.

Acknowledgements

The work at Dalhousie University was funded in part by grants from NSERC and the Office of Naval Research, and the work at the Freie Universität by the Deutsche Forschungsgemeinschaft through SFB 290.

References

[1] E. Bauer, H. Poppa, G. Todd, F. Bonczek, J. Appl. Phys. 45 (1974) 5164.
[2] E. Bauer, Appl. Phys. A 51 (1990) 71.
[3] D. Schlatterbeck, M. Parschau, K. Christmann, Surf. Sci. 418 (1998) 240.
[4] S.H. Payne, H.J. Kreuzer, A. Pavlovska, E. Bauer, Surf. Sci. 345 (1996) L1.
[5] M. Parschau, K. Christmann, Ber. Bunsenges. Phys. Chem. 99 (1995) 1376.
[6] M. Parschau, D. Schlatterbeck, K. Christmann, Surf. Sci. 376 (1997) 133.
[7] S.H. Payne, H.J. Kreuzer, Surf. Sci. 399 (1998) 135.
[8] W. Widdra, P. Trischberger, W. Friess, D. Menzel, S.H. Payne, H.J. Kreuzer, Phys. Rev. B 57 (1998) 4111.
[9] S.H. Payne, H.J. Kreuzer, Surf. Sci. 338 (1995) 261.
[10] H.J. Kreuzer, S.H. Payne, Theoretical approaches to the kinetics of adsorption, desorption and reactions at surfaces, in: M. Borowko (Ed.), Computional Methods in Colloid and Interface Science, Marcel Dekker Inc., New York, 1999.
[11] C. Stampfl, M. Scheffler, H. Pfnür, H.J. Kreuzer, S.H. Payne, Phys. Rev. Lett. 83 (1999) 2993.
[12] Such calculations can be done routinely, for instance, with the ASTEK program package for the Analysis and Simulation of Thermal Equilibrium and Kinetics of gases adsorbed on solid surfaces, written by H.J. Kreuzer, S.H. Payne, Available from Helix Science Applications, 618 Ketch Harbour Road, Portuguese Cove, N.S. B3V 1K1 Canada.
[13] D.A. King, T.E. Madey, J.T. Yates Jr., J. Chem. Phys. 55 (1971) 3236.
[14] E. Bauer, F. Bonczek, H. Poppa, G. Todd, Surf. Sci. 53 (1975) 5164.
[15] E. Habenschaden, J. Küppers, Surf. Sci. 138 (1984) L147.
[16] H.J. Kreuzer, S.H. Payne, Surf. Sci. 222 (1989) 404.
[17] R.N. Carter, A. Brad Anton, J. Vac. Sci. Technol. A 10 (1992) 344.